

Enhanced superelasticity and reversible elastocaloric effect in nano-grained NiTi alloys with low stress hysteresis

Min Zhou, Wei Wang, Haojian Su, Zhongjun Hu, and Laifeng Li

Citation: Chin. Phys. B, 2024, 33 (**5**): 056501. DOI: 10.1088/1674-1056/ad2a75
Journal homepage: http://cpb.iphy.ac.cn; http://iopscience.iop.org/cpb

What follows is a list of articles you may be interested in

Elastocaloric effect and mechanical behavior for NiTi shape memory alloys

Min Zhou(周敏), Yu-Shuang Li(李玉霜), Chen Zhang(张晨), Lai-Feng Li(李来风)
Chin. Phys. B, 2018, 27 (**10**): 106501. DOI: 10.1088/1674-1056/27/10/106501

Large elastocaloric effect in Ti-Ni shape memory alloy below austenite finish temperature

Xiao-Hua Luo(罗小华), Wei-Jun Ren(任卫军), Wei Jin(金伟), Zhi-Dong Zhang(张志东)
Chin. Phys. B, 2017, 26 (**3**): 036501. DOI: 10.1088/1674-1056/26/3/036501

Response of thermal source in a transversely isotropic thermoelastic half-space with mass diffusion by finite element method

Ibrahim A. Abbas, Rajneesh Kumar, Vijay Chawla
Chin. Phys. B, 2012, 21 (**8**): 084601. DOI: 10.1088/1674-1056/21/8/084601

Generalized thermoelsticity of the thermal shock problem in an isotropic hollow cylinder and temperature dependent elastic moduli

Ibrahim A. Abbas and Mohamed I. A. Othman
Chin. Phys. B, 2012, 21 (**1**): 014601. DOI: 10.1088/1674-1056/21/1/014601

Enhanced superelasticity and reversible elastocaloric effect in nano-grained NiTi alloys with low stress hysteresis

Min Zhou(周敏)[1,†], Wei Wang(王维)[2,‡], Haojian Su(苏浩健)[1], Zhongjun Hu(胡忠军)[1,§], and Laifeng Li(李来风)[1]

[1] *Key Laboratory of Cryogenic Science and Technology, Technical Institute of Physics and Chemistry, Chinese Academy of Sciences, Beijing* 100190, *China*
[2] *Songshan Lake Materials Laboratory, Dongguan* 523808, *China*

(Received 23 December 2023; revised manuscript received 6 February 2024; accepted manuscript online 19 February 2024)

Solid-state cooling technologies have been considered as potential alternatives for vapor compression cooling systems. The search for refrigeration materials displaying a unique combination of pronounced caloric effect, low hysteresis, and high reversibility on phase transformation was very active in recent years. Here, we achieved increase in the elastocaloric reversibility and decrease in the friction dissipation of martensite transformations in the superelastic nano-grained NiTi alloys obtained by cold rolling and annealing treatment, with very low stress hysteresis (6.3 MPa) under a large applied strain (5%). Large adiabatic temperature changes ($\Delta T_{max} = 16.3$ K at $\varepsilon = 5\%$) and moderate COP_{mater} values (maximum $COP_{mater} = 11.8$ at $\varepsilon = 2\%$) were achieved. The present nano-grained NiTi alloys exhibited great potential for applications as a highly efficient elastocaloric material.

Keywords: elastocaloric effect, stress hysteresis, superelasticity, NiTi alloy

PACS: 65.40.gd, 46.25.Hf, 62.20.fg **DOI:** 10.1088/1674-1056/ad2a75

1. Introduction

Refrigeration is a vital technology for modern society. However, the traditional vapor compression cooling technologies are facing more and more pressure because their refrigerating fluids have high global warming potential and severely damage the environment. The solid-state cooling technologies based on caloric effects (such as magnetocaloric, electrocaloric, elastocaloric, and barocaloric effect) are considered as promising alternatives for vapor compression cooling technology due to their environmentally friendly and efficient nature.[1] Among these solid-state cooling technologies, the elastocaloric refrigeration was evaluated to be the most potential way by the US Department of Energy owing to its higher cooling efficiency and wider working temperature range. Elastocaloric refrigeration could be characterized by the adiabatic temperature change (ΔT_{adi}) or the isothermal entropy change (ΔS_{iso}).[2] Furthermore, hysteresis reflected the energy dissipation during transformation, which was detrimental to the reversibility of transformation.[3–5] Low hysteresis was important for achieving high energy conversion efficiency and for enhancing the reversibility of transformation.[5–7] However, most elastocaloric materials showed the first-order phase transformation behavior, which caused the intrinsic and unavoidable stress hysteresis. In recent years, more works focused on narrowing down the stress hysteresis. Alloying moderate elements was reported to be an effective way to reduce the hysteresis behavior and to improve the mechanical properties.[8–13] Besides, the microstructural feature was also a decisive factor influencing the stress hysteresis.[14–21]

Compared with the common elastocaloric materials of the Cu-based[22,23] and the ferromagnetic alloys,[24–27] the NiTi-based alloys were studied and were considered as the most promising for practical applications owing to their excellent mechanical properties, large elastocaloric effect, and commercial availability.[28–33] However, large stress hysteresis could cause to large energy dissipation and to degradation of cyclic stability in the NiTi alloys.[34] In the present work, the nano-grained NiTi alloys with very low stress hysteresis were obtained by cold rolling and appropriately annealing treatment. The effects of grain size on the superelasticity, elastocaloric effect, and stress hysteresis were studied. Enhanced superelasticity and reversible elastocaloric effect were observed in the nano-grained NiTi alloys with low stress hysteresis.

2. Experimental details

The commercial austenitic NiTi sheets (Kelloggs Company) of 5-mm thickness ($A_f = -10$ °C) were used in this study. The NiTi sheets were sandwich packaged by stainless steel sheets and cold-rolled by multiple passes until 3.15-mm final thickness (37% thickness reduction) at room temperature. The cold-rolled sheets were wire-cut along the rolling direction and then annealed at different conditions to achieve different grain sizes (as shown in Table 1). The grain sizes were measured by a bright field TEM (JEOL model JEM 2010F) and a Williamson–Hall method. Uniaxial tensile tests were conducted on a electronic universal testing machine (Instron

†Corresponding author. E-mail: mzhou@mail.ipc.ac.cn
‡Corresponding author. E-mail: wangwei@sslab.org.cn
§Corresponding author. E-mail: zjhu@mail.ipc.ac.cn

© 2024 Chinese Physical Society and IOP Publishing Ltd

model 5985) with a electronic extensometer (Epsilon model 3542-025M-100-LT, with a gauge length of 25 mm). The isothermal tension was performed at a lower strain rate of 0.0001/s. For the elastocaloric measurement, the sample was loaded at a much higher strain rate of 0.02/s (approximately reach the adiabatic condition), and then held for 2 min–5 min to make sure the specimen temperature returned to the original value. The tests were conducted with a strain-controlled mode. The temperature changes during the testing process were monitored by a platinum resistance thermometer attached at the middle position of the sample. To improve thermal contact, the platinum resistance thermometer was attached using silver paint. The output of the platinum resistance thermometer was read by a multimeter (Keithley model 2000) at a frequency of 2 Hz. All measurements were carried out in air without any thermal insulation.

Table 1. Average grain size and mechanical properties.

Sample number	1	2	3	4	5
Annealing condition	Raw NiTi	250 °C/2 min	250 °C/30 min	350 °C/8 min	450 °C/5 min
Average grain size (nm)	–	4	12	31	63
Hysteresis loops ($\varepsilon = 3\%$) (MPa)	4.49	1.78	1.74	3.61	4.33
Phase transition stress ($\varepsilon = 3\%$) (MPa)	155	450	320	297	223
Young's modulus (GPa)	–	36.85	26.90	25.13	22.13

3. Results and discussion

Figure 1 showed a set of representative TEM images obtained after the cold rolling and annealing treatment. The average grain size of the sample #2 was 4 nm, showing that appropriately annealing (at 250 °C for 2 min) promoted recovery of the deformed lattice and resulted in fine grain. With increasing annealing temperature and time, the grain sizes grown up and reached to 63 nm for the sample #5 annealed at 450 °C for 5 min (as shown in Table 1).

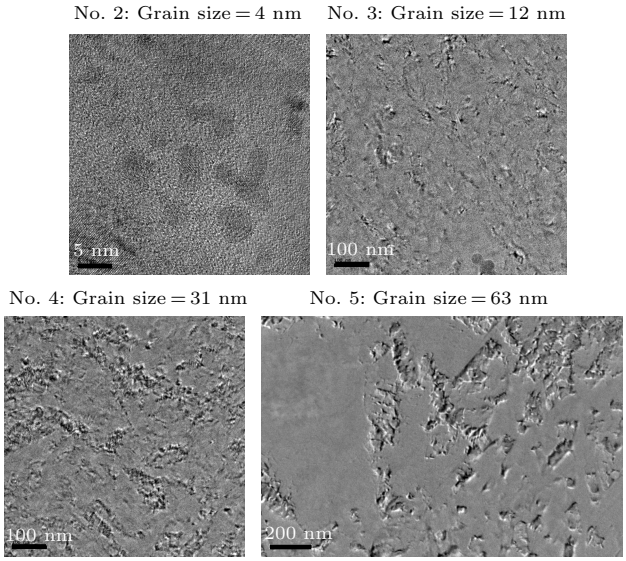


Fig. 1. TEM imagines of the annealed NiTi alloys with different grain sizes.

The isothermal stress–strain curves were summarized in Fig. 2. The tensile test was controlled by the strain mode with a low strain rate of 0.0001/s to satisfy the isothermal condition. For the raw NiTi austenite alloy (sample #1) with the applied strain of 1%, the stress linearly increased with strain, corresponding to the elastic response of the austenite phase. Then a relatively flat 'plateau' appeared in the stress–strain curve, which corresponded to the stress-induced martensite transformation. After the stress was released, the strain recovered, indicating the superelastic deformation. With increasing the applied strain, larger residual strain was observed. The residual strain even increased to about 2.3% when the applied strain enhanced to 3%, showing amount of remnant martensite stabilized by dislocation strain field.[35] With increasing the applied strain to over 3%, the sample fractured. These results showed that the raw NiTi alloy did not possess good superelastic performance. It was interesting that the excellent superelastic properties were obtained by cold-rolling and appropriately annealing treatment. For the annealed sample #2 with fine grain size of 4 nm, the stress–strain relation showed ideal superelastic behavior and small stress hysteresis loop between the loading and unloading curves in a wide strain range of 5%. Only a little amount of residual strain of 0.1% was observed even at high strain level of 5%, which was much lower than that of the raw NiTi alloy. The stress hysteresis loop between the loading and unloading curves increased with increasing strain levels and attained to just 6.3 MPa at the applied strain of 5%, which was much lower than that of most elastocaloric materials.[11,22,29,36,37] With increasing the grain sizes, the annealed samples showed superelastic deformation in smaller strain ranges. When the grain size increased to 63 nm (annealing at 450 °C for 5 min), large amount of residual strain of 2% was observed at the applied strain level of 3%, showing deteriorative superelastic deformation. This result was analogous to that of the raw NiTi alloy.

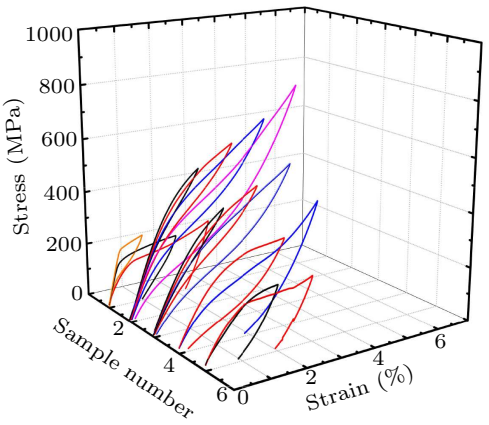


Fig. 2. The isothermal stress–strain curves of all the samples (#1: the raw NiTi alloy; #2: annealed at 250 °C for 2 min; #3: annealed at 250 °C for 30 min; #4: annealed at 350 °C for 8 min; #5: annealed at 450 °C for 5 min).

In order to fully study the superelastic properties of the NiTi alloys with different grain sizes, the isothermal stress–strain curves with the applied strain of 3% were shown in Fig. 3. The sample #2 with small grain size of 4 nm showed nonlinear superelastic behavior with high phase transition stress (450 MPa) and small hysteresis loop (1.78 MPa). With increasing grain sizes, the phase transition stress decreased to 200 MPa and hysteresis loop area slightly enhanced to 5.5 MPa for the annealed sample #5 with grain size of 63 nm (as shown in Fig. 3 and in Table 1), which got close to those of the raw NiTi alloy. These results showed that fine grains were beneficial for lower phase transition hysteresis and higher phase transition stress. The generation of internal stress with increasing grain size was favorable for the formation of the stress-induced martensite phase, leading to the gradual degradation of the critical phase transition stress.[38,39] To illustrate the effect of grain sizes on the stress hysteresis in a simple way, a multiscale model was reported. The variation of hysteresis loop area (H) was approximated by a simple scaling law as[14,40]

$$H = H_0(1 - l_{\mathrm{m}}/l), \tag{1}$$

where H_0 is the hysteresis loop area of the coarse-grained poly-crystal, l_{m} is the austenite/martensite interface thickness, and l is the grain size. From Eq. (1), the H value decreased with reducing grain size. When the grain size decreased to the interface thickness ($l = l_{\mathrm{m}}$), the stress linearly increased with strain, corresponding to the linear superelasticity. From thermodynamics point of view, the macroscopic stress hysteresis of a polycrystalline material meant mechanical energy dissipation in a phase transition process.[40] So, the stress hysteresis greatly affected the energy conversion efficiency. The low stress hysteresis of these nano-grained NiTi alloys was important for achieving high efficiency.

The Young's moduli were also obtained (as shown in Fig. 3 and Table 1). For the annealed samples, the Young's modulus decreased with increasing grain sizes. It was reported that the Young's modulus of grain boundary and amorphous phase were significantly higher than that of the crystallite in NiTi alloys.[41–43] Therefore, the Young's modulus decreased with increasing grain sizes, which may be related to the nucleation, growth, and the resultant decrease of the volume fraction of grain boundary.

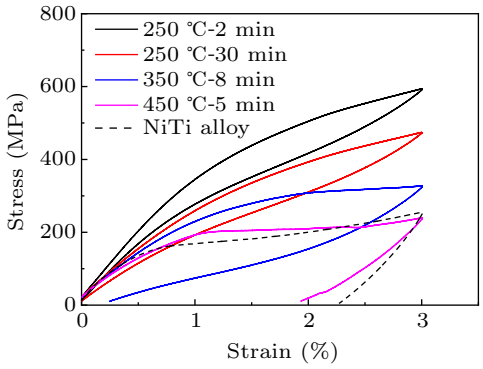


Fig. 3. The isothermal stress–strain curves of all the samples with the applied strain of 3%.

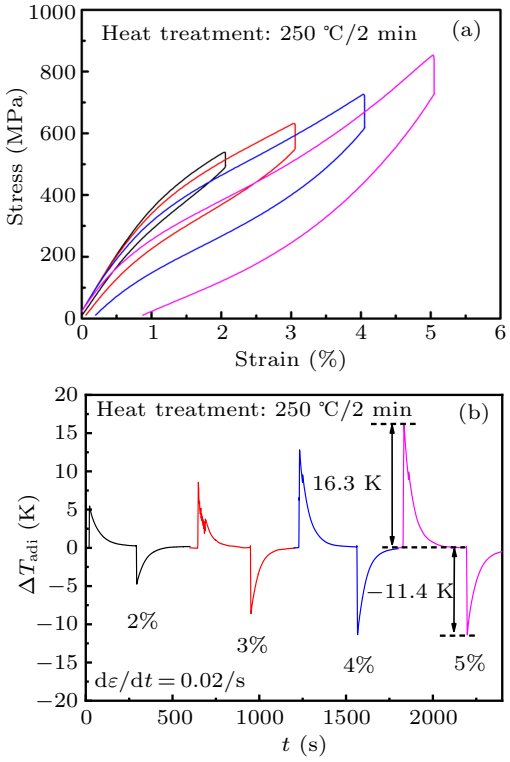


Fig. 4. (a) The adiabatic stress–strain curves ($\mathrm{d}\varepsilon/\mathrm{d}t = 0.02$/s), (b) the measured ΔT_{adi} values of the annealed sample #2 with grain size of 4 nm.

Figure 4 shows the adiabatic stress–strain curves and the corresponding temperature changes (ΔT_{adi}) of the sample #2. The absolute temperature changes ($|\Delta T_{\mathrm{adi}}|$) during both loading and unloading enhanced with increasing the applied strain levels, which maybe due to the increase in the volume fraction of stress-induced martensitic transformation and reverse transformation. It was worth noting that the absolute temperature changes ($|\Delta T_{\mathrm{adi}}|$) upon loading were almost equal to those

upon unloading process in the applied strain range of 2%–4%, showing reversible elastocaloric behavior. When the applied strain increased to 5%, a maximum ΔT_{adi} value increased to 16.3 K upon loading but decreased to −11.4 K upon unloading. Considering the mentioned low stress hysteresis, the moderate ΔT_{adi} value is competitive compared with other elastocaloric materials.[22,36,37] As shown in Fig. 4(a), the residual strain increased to about 1% when the applied strain increased to 5%, showing that increased remnant martensite was stabilized by dislocations and was not fully reversible any more. So, the increased residual martensite hindered the decrease of $-\Delta T_{adi}$ values at $\varepsilon = 5\%$.

To study the effect of grain size on the elastocaloric effect of the present NiTi alloys, the adiabatic temperature changes (ΔT_{adi}) were measured with the applied strain of 3% and were shown in Fig. 5. Upon loading, the measured ΔT_{adi} value of the fine-grained sample #2 reached to its maximum value of 9 K due to the release of heat during the forward martensite transformation. During holding, the sample temperature recovered to room temperature as a result of heat exchange between the sample and environment. Then ΔT_{adi} value decreased to −9 K upon unloading due to the absorption of heat during reverse martensite transformation. Finally, the sample temperature recovered again to room temperature. The measured ΔT_{adi} value upon loading was almost equal to that upon unloading, indicating the elastocaloric reversibility ($\Delta T_{load} = \Delta T_{unload}$) between the forward and reverse martensite transformations for the nano-grained NiTi alloys. The elastocaloric reversibility had scarcely been reported in the NiTi-based elastocaloric materials due to the friction dissipation of martensite transformations. In the present work, the very low stress hysteresis of the nano-grained NiTi alloys greatly decreased the friction dissipation of martensite transformations, causing the elastocaloric reversibility and increasing the energy conversion efficiency of the elastocaloric effect.

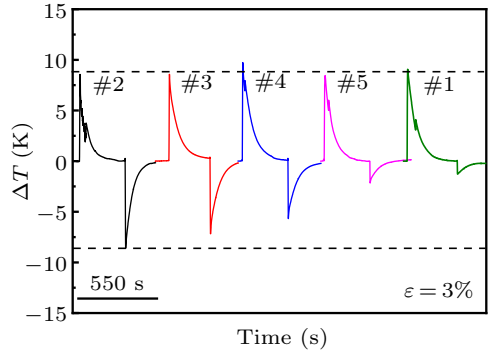


Fig. 5. The measured ΔT_{adi} values as a function of time for all the samples.

With increasing the grain sizes, the measured ΔT_{adi} values upon loading were almost equal to that of the fine-grained sample #2, indicating that grain sizes hardly affected the ΔT_{adi} values. However, the elastocaloric irreversibility ($\Delta T_{irr} = \Delta T_{load} - \Delta T_{unload}$) occurred and increased with increasing the grain sizes. When the average grain size increased to 63 nm, the elastocaloric irreversibility of the sample #5 nearly reached to that of the raw NiTi alloy. The increased residual strain with increasing grain sizes (as shown in Fig. 3) hindered superelastic deformation and decreased adiabatic temperature change upon unloading process. Besides, the enhanced stress hysteresis (as shown in Table 1) could also contribute to the increased elastocaloric irreversibility.

The COP_{mat} ($= Q/W$, the coefficient-of-performance of the material) was another key parameter to evaluate the caloric performance of the elastocaloric materials.[8,29,44–46] Since the elastocaloric refrigeration employed the heat absorption process during unloading, the measured ΔT_{adi} value during unloading was used to estimate the absorbed heat Q ($= \Delta T_{adi} C_p \rho$). The input work ($W$) corresponded to the stress hysteresis loop area (H), which could be obtained by integrating the area enclosed by the loading and the unloading trajectories in the adiabatic stress–strain curves. With the applied strain of 2%–5%, the COP_{mater} values of the fine-grained sample #2 were estimated by using the measured density ($\rho = 6.8$ g/cm^3) and heat capacity ($C_p = 424$ J/(kg·K)) and shown in Fig. 6. The COP_{mater} value was calculated to be 11.8 with the applied strain of 2%, which was much higher than those of many poly-crystalline NiTi alloys.[47] These results showed that the low stress hysteresis of the annealed nano-grained NiTi alloys contributed to high COP_{mater} value and energy conversion efficiency. With increasing the applied strain, the COP_{mater} values showed an inverse dependency on the applied strain level. Considering the adiabatic temperature change and superelastic performance mentioned above, appropriate strains and COP_{mater} values would be expected in actual applications.

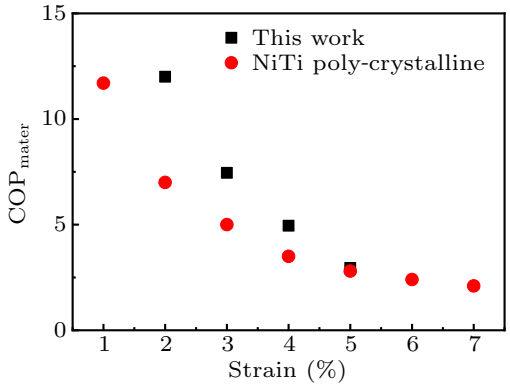


Fig. 6. The COP_{mater} values of the fine-grained sample #2. Red solid circle symbols correspond to literature data.[45]

To further evaluate the comprehensive elastocaloric properties, the cooling performance data (ΔT_{adi}, COP_{mat}, and stress hysteresis) of the nano-grained NiTi alloys (with the applied strain of 2%–5%) and other literatures[5,22,25,26,28,36,48–51]

were shown in Fig. 7. Among the collected diverse alternatives, the FePd-based alloys showed low stress hysteresis but small ΔT_{adi}, the common NiTi-based alloys possessed large ΔT_{adi}, COP_{mat} values but high stress hysteresis. These results indicated that there was still considerable space to improve refrigeration performances by material engineering. By moderate cold-rolling and annealing treatment, the nano-grained NiTi alloys showed not only large adiabatic temperature changes (-11.4 K upon unloading), moderate COP_{mater} values (11.8 at $\varepsilon = 2\%$) but also low stress hysteresis (several MPa).

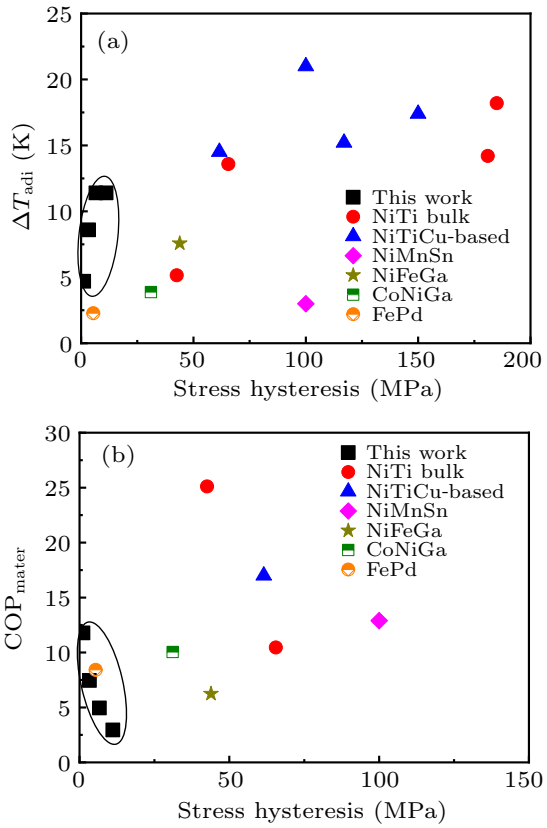


Fig. 7. Comparison of cooling performance between the present nano-grained NiTi alloys and other elastocaloric materials:[5,22,25,26,28] (a) the $|\Delta T_{adi}|$ values during unloading, (b) the COP_{mater} values *versus* the stress hysteresis.

4. Conclusions

In summary, the nano-grained NiTi alloys were obtained by cold-rolling and appropriately annealing treatment. Compared with the raw NiTi alloys, the annealed nano-grained NiTi alloys show excellent superelasticity and reversible elastocaloric properties. Large adiabatic temperature changes ($\Delta T_{max} = 16.3$ K) and moderate COP_{mater} values (maximum $COP_{mater} = 11.8$ at $\varepsilon = 2\%$) are achieved. What is more, the very low stress hysteresis (several MPa) of the nano-grained NiTi alloy greatly decreases the friction dissipation of martensite transformations, causing to the elastocaloric reversibility and to increase in the energy conversion efficiency. The nano-grained NiTi alloys exhibit great potential for applications as a highly efficient room-temperature elastocaloric material.

Acknowledgements

Project supported by the Science Fund of the Key Laboratory of Cryogenic Science and Technology (Grant Nos. CRYO20230203 and CRYO202106), the National Natural Science Foundation of China (Grant Nos. 51872299 and 52071223), the National Key Research and Development Program of China (Grant No. 2019YFA0704904).

References

[1] Crossley S, Mathur N D and Moya X 2015 *AIP Advances* **5** 067153
[2] Manosa L, Planes A and Acet M 2013 *J. Mater. Chem. A* **1** 4925
[3] Wu Y, Ertekin E and Sehitoglu H 2017 *Acta Mater.* **135** 158
[4] Liu D M, Cong D Y, Sun X M, Chen H Y, Nie Z H, Chen Z, Zhang Y, Zhu C, Qu Y H, Zhu J and Wang Y D 2017 *J. Alloys Compd.* **728** 655
[5] Tusek J, Engelbrecht K, Millán-Solsona R, Mañosa L, Vives E, Mikkelsen L P and Pryds N 2015 *Adv. Energy Mater.* **5** 1500361
[6] Chluba C, Ge W W, Miranda R LStrobel J L, Kienle L, Quandt E and Wuttig M 2015 *Science* **348** 1004
[7] Song Y, Chen X, Dabade V, Shield T W and James R D 2013 *Nature* **502** 85
[8] Yang Z, Cong D Y, Yuan Y, Li R G, Zheng H X, Sun X M, Nie Z H, Ren Y and Wang Y D 2020 *Appl. Mater. Today* **21** 100844
[9] Li D, Li Z, Zhang X, Yang B, Wang D, Zhao X and Zuo L 2020 *Scripta Mater.* **189** 78
[10] Ijaz M F, Kim H Y, Hosoda H and Miyazaki S 2014 *Scripta Mater.* **72–73** 29
[11] Ma Y, Jiang C, Li Y, Xu H, Wang C and Liu X 2007 *Acta Mater.* **55** 1533
[12] Villa E, Villa E, D'Eril M M, Nespoli A and Passaretti F 2018 *J. Alloys Compd.* **763** 883
[13] Wang J, Wang H and Jiang C 2013 *Mater. Sci. Eng. A-Struct.* **578** 256
[14] Sun Q P and He Y J 2008 *Int. J. Solids Struct.* **45** 3868
[15] Zhu X, Zhang X and Qian M 2018 *AIP Advances* **8** 125002
[16] Lu B, Song M, Zhou Z, Liu W, Wang B, Lu S, Wu C, Yang L and Liu J 2019 *J. Alloys Compd.* **785** 1023
[17] Zhu X, Zhang X, Qian M and Imran M 2019 *J. Alloys Compd.* **792** 780
[18] Shi X B, Guo F M, Zhang J S, Ding H L and Cui L S 2016 *J. Alloys Compd.* **688** 62
[19] Zhao D, Liu J, Chen X, Sun WLi Y, Zhang M, Shao Y, Zhang H and Yan A 2017 *Acta Mater.* **133** 217
[20] Huang X M, Wang L D, Liu H X, Yan H L, Jia N, Yang B, Li Z B, Zhang Y D, Esling C, Zhao X and Zuo L 2019 *Intermetallics* **113** 106579
[21] Yuan B, Zhu X, Zhang X and Qian M 2019 *J. Mater. Sci.* **54** 9613
[22] Manosa L, Jarque-Farnos S, Vives E and Planes A 2013 *Appl. Phys. Lett.* **103** 211904
[23] Vives E, Burrows S, Edwards R S, Dixon S, Mañosa L, Planes A and Romero R 2011 *Appl. Phys. Lett.* **98** 011902
[24] Manosa L, González-Alonso D, Planes A, Bonnot E, Barrio M, Tamarit J L, Aksoy S and Acet M 2010 *Nat. Mater.* **9** 478
[25] Yang Z, Cong D Y, Huang L, Nie Z H, Sun X M, Zhang Q H and Wang Y D 2016 *Mater. Design* **92** 932
[26] Sun W, Liu J, Lu B, Li Y and Yan A 2016 *Scripta Mater.* **114** 1
[27] Huang Y J, Hu Q D, Bruno N M, Chen J H, Karaman I, Ross Jr J H and Li J G 2015 *Scripta Mater.* **105** 42
[28] Bechtold C, Chluba C, Miranda R L and Quandt E 2012 *Appl. Phys. Lett.* **101** 091903
[29] Cui J, Wu Y, Muehlbauer J, Hwang Y, Radermacher R, Fackler S, Wuttig M and Takeuchi I 2012 *Appl. Phys. Lett.* **101** 073904
[30] Kirsch S M, Welsch F, Michaelis N, Schmidt M, Wieczorek A, Frenzel J, Eggeler G, Schütze A and Seelecke S 2018 *Energy Technology* **6** 1567
[31] Ossmer H, Lambrecht F, Gultig M, Chluba C, Quandt E and Kohl M 2014 *Acta Mater.* **81** 9
[32] Tusek J, Engelbrecht K, Mikkelsen L P and Pryds N 2015 *J. Appl. Phys.* **117** 124901

[33] Liang X, Xiao F, Jin M, Jin X, Fukuda T and Kakeshita T 2017 *Scripta Mater.* **134** 42
[34] Zhou M, Li Y, Zhang C, Li S, Wu E, Li W and Li L 2018 *J. Phys. D: Appl. Phys.* **51** 135303
[35] Cong D Y, Saha G and Barnett M R 2014 *Acta Biomater.* **10** 5178
[36] Bonnot E, Romero R, Manosa L, Vives E and Planes A 2008 *Phys. Rev. Lett.* **100** 125901
[37] Cong D, Xiong W, Planes A, Ren Y, Manosa L, Cao P, Nie Z, Sun X, Yang Z, Hong X and Wang Y 2019 *Phys. Rev. Lett.* **122** 255703
[38] Xiao F, Fukuda T, Jin X, Liu J and Kakeshita T 2018 *Phys. Status Solidi B* **255** 1700246
[39] Chen H, Xiao F, Liang X, Li Z, Jin X and Fukuda T 2018 *Acta Mater.* **158** 330
[40] Ahadi A and Sun Q 2013 *Appl. Phys. Lett.* **103** 021902
[41] Liu Y and Xiang H 1998 *J. Alloys Compd.* **270** 154
[42] Tsuchiya K, Hada Y, Koyano T, Nakajima K, Ohnuma M, Koike T, Todaka Y and Umemoto M 2009 *Scripta Mater.* **60** 749
[43] Xia M, Liu P and Sun Q 2018 *Mater. Lett.* **211** 352
[44] Xiao F, Jin M, Liu J and Jin X 2015 *Acta Mater.* **96** 292
[45] Zhang K, Kang G and Sun Q 2019 *Scripta Mater.* **159** 62
[46] Chen J, Zhang K, Kan Q, Yin H and Sun Q 2019 *Appl. Phys. Lett.* **115** 093902
[47] Zhou M, Li Y S, Zhang C and Li L F 2018 *Chin. Phys. B* **27** 106501
[48] Chen J, Xing L, Fang G, Lei L and Liu W 2021 *Acta Mater.* **208** 116741
[49] Shen A, Zhao D, Sun W, Liu J and Li C 2017 *Scripta Mater.* **127** 1
[50] Xiao F, Fukuda T and Kakeshita T 2013 *Appl. Phys. Lett.* **102** 161914
[51] Li Y, Zhao D and Liu J 2016 *Sci. Rep.* **6** 25500